Journal of Hazardous Materials 221–222 (2012) 242–247

Contents lists available at SciVerse ScienceDirect

Journal of Hazardous Materials

journal homepage: www.elsevier.com/locate/jhazmat

Different families of volatile organic compounds pollution control by microporous carbons in temperature swing adsorption processes

Shivaji G. Ramalingam[a,*], Pascaline Pré[a], Sylvain Giraudet[b,c], Laurence Le Coq[a], Pierre Le Cloirec[b,c], Olivier Baudouin[d], Stéphane Déchelotte[d]

[a] Ecole des Mines de Nantes, GEPEA, UMR-CNRS 6144,4 rue Alfred Kastler, BP20722, 44307 Nantes, Cedex 03, France
[b] Ecole Nationale Supérieure de Chimie de Rennes, CNRS, UMR 6226, Avenue du General Leclerc, CS 50837 35708 Rennes, Cedex 7, France
[c] Université Européenne de Bretagne,France
[d] PROSIM, Stratège Bâtiment A, BP 27210, F-31672 Labege, Cedex, France

ARTICLE INFO

Article history:
Received 8 February 2012
Received in revised form 12 April 2012
Accepted 16 April 2012
Available online 21 April 2012

Keywords:
Microporous activated carbon
VOC
Adsorption
Hot nitrogen regeneration

ABSTRACT

In this research work, the three different VOCs such as acetone, dichloromethane and ethyl formate (with corresponding families like ketone, halogenated-organic, ester) are recovered by using temperature swing adsorption (TSA) process. The vapors of these selected VOCs are adsorbed on a microporous activated carbon. After adsorption step, they are regenerated under the same operating conditions by hot nitrogen regeneration. In each case of regeneration, Factorial Experimental Design (FED) tool had been used to optimize the temperature, and the superficial velocity of the nitrogen for achieving maximum regeneration efficiency (R_E) at an optimized operating cost ($OP_€$). All the experimental results of adsorption step and hot nitrogen regeneration step had been validated by the simulation model PROSIM. The average error percentage between the simulation and experiment based on the mass of adsorption of dichloromethane was 3.1%. The average error percentages between the simulations and experiments based on the mass of dichloromethane regenerated by nitrogen regeneration were 4.5%.

1. Introduction

Volatile organic compounds (VOCs) like dichloromethane, acetone and ethyl formate are widely used in the oil sands process to extract the bitumen from the oil sands [1]. Acetone and ethyl formate have adverse toxic effects on human central nervous system and environment [2]. And dichloromethane even causes cancer to humans and so the European States have decided to ban the use of it for concentration equal to or greater than 0.1 by mass percent [2]. This research work focuses on the removal of VOCs by adsorption using commercial microporous activated carbon and then regenerates the adsorbed phase. Many studies have been made on the influence of the operating conditions of adsorption phase [3–7]. But, there are no studies made on the influence of operating conditions of regeneration of different families of VOCs as a function of regeneration efficiency (R_E) and the operating cost ($OP_€$). Factorial Experimental Design (FED) is an effective design tool to understand the influence of each operating condition (such as flow rate and the temperature of the hot nitrogen) on the regeneration efficiency (R_E) and the operating cost ($OP_€$) [8]. The dynamic experiments of adsorption and regenerations will be validated by using the simulation model PROSIM [9–11].

The objectives of this research work are: (1) characterize the microporous activated carbon (CECA – ACV 404) and establish the isotherm equilibrium data for different VOCs – activated carbon system; (2) design dynamic hot nitrogen regeneration experiments for 3 VOCs – ACV 404 systems by FED (VOCs – acetone, dichloromethane, and ethyl formate); (3) compare the regeneration performance of different families of VOCs – activated carbon system under same hot regeneration operating conditions by FED results of ANOVA equation.

2. Simulation model

The cyclic adsorption–desorption process is simulated by solving the mass and energy balances during each step: adsorption, possibly bed preheating by the walls, thermal desorption by steam or nitrogen flow, and/or desorption under vacuum. The main equations and assumptions used are described below [11,12].

2.1. Mass balance

The partial mass balance equation expresses that the change in the concentration of the VOC in the gas phase along the column

* Corresponding author. Tel.: +33 633923537.
E-mail address: shivaji.ramalingam@yahoo.co.in (S.G. Ramalingam).

0304-3894/$ – see front matter © 2012 Elsevier B.V. All rights reserved.
http://dx.doi.org/10.1016/j.jhazmat.2012.04.037

Nomenclature

a_p	ratio between the external surface and the volume of the particle (m^{-1})
bo	parameter of the model (atm^{-1})
b_1	parameter of the model (T^{-1})
Cp_a	specific heat capacity of adsorbed phase ($J\,kg^{-1}\,K^{-1}$)
Cp_p	specific heat capacity of the adsorbent ($J\,kg^{-1}\,K^{-1}$)
C_i	VOC concentration in the gas phase, ($mol\,m^{-3}$)
Cp_g	specific heat capacity of gas phase ($J\,kg^{-1}\,K^{-1}$)
D_L	axial mass dispersion coefficient ($m^2\,s^{-1}$)
D_{gl}	global mass transfer coefficient ($m^2\,s^{-1}$)
d_c	diameter of the column (m)
D_L	diffusivity ($m^2\,s^{-1}$)
D_H	axial heat dispersion coefficient ($J\,m^{-1}\,s^{-1}$)
d_p	equivalent particle diameter (m)
e	thickness of the column (m)
H	enthalpy of gas phase ($J\,kg^{-1}$)
h_w	heat transfer coefficient of wall ($W\,m^2\,K^{-1}$)
h_p	heat transfer coefficient with solid particle ($W\,m^2\,K^{-1}$)
ΔH_i	enthalpy of adsorption/desorption of the compound i ($J\,mol^{-1}$)
ΔH_{vap}	latent heat of vaporization ($kJ\,mol^{-1}$)
K_f	external mass transfer coefficient ($m\,s^{-1}$)
K	global mass transfer coefficient (s^{-1})
PI	VOC ionization potential (eV)
P_i	equilibrium VOC partial pressure (atm)
q_i	adsorbed VOC concentration ($mol\,kg^{-1}$)
qi^*	adsorbed VOC concentration at the equilibrium with the gas phase ($mol\,kg^{-1}$)
q_i^*	VOC adsorbed quantity at the equilibrium ($mol\,kg^{-1}$)
q_{imo}	parameter of the model ($mol\,kg^{-1}$)
q_{m1}	parameter of the model (T^{-1})
q_i	VOC concentration in the adsorbed phase ($mol\,kg^{-1}$)
r_p	partcicle equivalent radius (m)
r_{mic},	adsorbent average micropore opening (nm).
T	temperature of gas (°C)
T_p	temperature of solid particle (°C)
v	superficial velocity ($m\,s^{-1}$)
V_m	molar VOC volume ($m^3\,mol^{-1}$)
v	superficial gas velocity ($m\,s^{-1}$)
y	VOC molar fraction in the gas
ρ_p	bulk adsorbent density ($kg\,m^{-3}$)
ρ_g	density of gas phase, ($kg\,m^{-3}$)
ε	bed porosity
λ	thermal conductivity of the material of the column (W/m/K)α – VOC polarizability ($10^{-24}\,cm^3$)
γ	surface tension of the liquid solvent ($mN\,m^{-1}$)
μ	kinematic viscosity (Pa s)

results from its transport in the gas flow and from the accumulation of the adsorbate in the solid phase

$$-D_L\frac{\partial^2 C_i}{\partial z^2}+\frac{\partial(vC_i)}{\partial z}+\frac{\partial C_i}{\partial t}+\frac{1-\varepsilon}{\varepsilon}\rho_p\frac{\partial q_i}{\partial t}=0 \quad (1)$$

2.2. Linear driving force model (LDF)

The adsorption or desorption kinetics is described according to the linear driving force model:

$$\frac{\partial q_i}{\partial t}=K\cdot(q_i^*-q_i) \quad (2)$$

Table 1
Langmuir isotherm coefficients results.

Langmuir model coefficients – VOC/ACV404 system				
VOCs	q_{m0} ($mol\,kg^{-1}$)	q_{m1} (T^{-1})	k_1 (T^{-1})	k_0 (atm^{-1})
Acetone	2.79	173	4810	7.8E−05
Ethyl formate	3.02	243	3893	1.6E−04
Dichloromethane	3.52	279	3087	4.0E−03

The overall resistance to the mass transfer between the gas and the solid phases embodies the partial resistance to the mass transfer at the external surface of the particles and the internal mass transfer resistance, expressed as a function of an effective diffusion coefficient D_{gl}:

$$\frac{1}{K}=\frac{\rho_p V_m q_i^*}{K_f a_p y}+\frac{r_p}{5D_{gl}a_p} \quad (3)$$

The external mass transfer coefficient K_f was derived from the correlation from Petrovic and Thodos. The effective diffusion coefficient takes into account the various diffusion mechanisms which control the migration of the organic component to the adsorption sites (porous, Knudsen, and surface diffusion). It is considered as an adjustable parameter. As a first approximation, effective the mass transfer resistance data was considered to be unchanged in the desorption step.

2.3. Equilibrium model

The value q_i^* in the linear driving force model (LDF) is computed from the modified Langmuir isotherm model, which takes into account the temperature effect on the equilibrium data. The parameters of the Langmuir equation were derived from the experimental data measured for the system (dichloromethane – ACV 404/acetone – ACV 404/ethyl formate – ACV 404) at 20, 40, 60 and 80 °C. The R-Stat statistical software was used to check the significance of the computed parameters using an interval of confidence of 95% by student t-test [11–13]. The results are summarized in Table 1 [14].

$$q_i^*=\frac{q_{m0}\exp(q_{m1}/T)b_0\exp(b_1/T)P_i}{1+b_0\exp(b_1/T)P_i} \quad (4)$$

2.4. Enthalpy balances

- In the gas phase:

$$-\rho_g D_L\frac{\partial^2 H}{\partial z^2}+\varepsilon\rho_g\frac{\partial H}{\partial t}+\varepsilon\frac{\partial(v\rho_g H)}{\partial z}+\frac{4}{d_c}\left[\frac{1}{hp}+\frac{dc.e}{(dc+e).\lambda}\right]^{-1}\times(T-T_w)+(1-\varepsilon)\frac{6h^p}{d_p}(T-T_p)=0 \quad (5)$$

- In the solid phase:

$$(\rho_p Cp_p+\rho_p Cp_a q_i)\frac{\partial T_p}{\partial t}+\frac{6h^p}{d_p}(T_p-T)+\Delta H_i\rho_p\frac{\partial q_i}{\partial t}=0 \quad (6)$$

The adsorption enthalpy was derived according to the following statistical predictive model [15]:

$$-\Delta H_{ads}=103.2+1.16\alpha+0.76\Delta H_{vap}-3.87PI-0.7\gamma-26.19r_{mic} \quad (7)$$

As a first approximation, the integral enthalpy of desorption was assumed to be equal to the one computed for the adsorption.

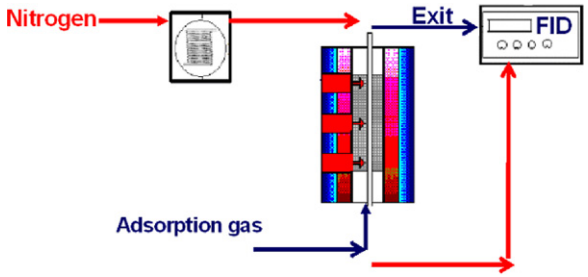

Fig. 1. Temperature swing adsorption (TSA) setup.

2.5. Ergun's pressure drop equation

$$\frac{\partial P}{\partial z} + 150 \times 10^{-5} \left(\frac{1-\varepsilon}{\varepsilon}\right)^2 \frac{\mu}{d_p^2} v + 1.75 \times 10^{-5} \left(\frac{1-\varepsilon}{\varepsilon}\right) \frac{\rho_g}{d_P} v^2 = 0 \quad (8)$$

The effect of pressure drop on the dynamic behavior of the adsorption and regeneration steps has been considered in the simulation model by Ergun's equation.

3. Experimental

3.1. Characterization of activated carbon

The activated carbon was activated physically by using steam for 40 min. The size of the carbon grain is 4 mm. The raw material of the activated carbon is coconut. The physical properties of the activated carbon (CECA – ACV404) such as B.E.T. surface specific area, micro pore volume (by Horvath–Kawazoe method), micropore average width (by Horvath–Kawazoe method) were measured by nitrogen adsorption isotherm at 77 K (Micromeritics ASAP 2010) [16]; the mesopore and macropore volume, and bulk density were measured by using mercury porosimeter (Micromeritics Autopore IV 9500) [17,18]. The properties resumed in the Table 2 were used in simulation models of adsorption and regeneration. The properties resumed in the Table 2 are used in simulation models of adsorption and regeneration.

3.2. Temperature swing adsorption (TSA) setup

Fig. 1 shows the experimental setup of temperature swing adsorption (TSA). It has an adsorption column with the dimension of 0.275 m high × 0.05 m internal diameter. Thermal couples are located at 3 various ports (at 2 cm, 19 cm and 25 cm from the top of the column) in the column to record the temperature data during adsorption and regeneration cycles. In the event to avoid heat losses, the column was insulated by 2 cm thick glass wool. During the adsorption step, 30 g m^{-3} of VOC concentration (acetone, dichloromethane and ethyl formate) is prepared by the VOC generating 25.8 °C. The concentration of the VOC was measured and calibrated by using by a commercial Flame Ionization Detector (FID) called CAMBUSTION HFR-400FFID. For the calibration curve, different volume samples (from 10 to 400 μl) are injected into a glass balloon of 1 L volume. The mass of VOC is calculated by multiplying density of VOC and volume of VOC injected in the glass balloon. Once having the value of VOC mass, the concentration (g m^{-3}) is calculated by the ratio of mass of VOC to the volume of the glass balloon. Hence, a linear calibration curve of concentration of VOC (g m^{-3}) vs FID response (volts) could be established for the dynamic experiments. The superficial velocities of the adsorption gas corresponding to acetone, ethyl formate and dichloromethane are 0.24, 0.23 and 0.26 m s^{-1} respectively.

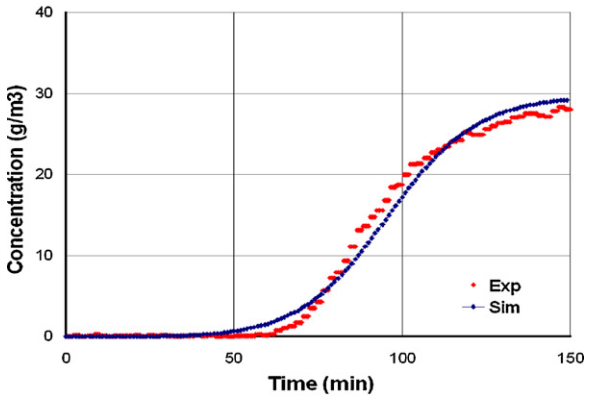

Fig. 2. Ethyl formate breakthrough profile of experiment and simulation.

Once after the adsorption step, the activated carbon is regenerated by hot nitrogen. FED has allowed to construct 2 × 2 design by changing the operating conditions such as temperature of the nitrogen in the range [130 < T < 170 °C] and the superficial velocity of the nitrogen in the range [0.10 < v < 0.17 m s^{-1}]. By doing analysis of variance (ANOVA) for the four experiments of regenerations with the statistical analysis software MINITAB, the regeneration efficiency (R_E) and the operating cost ($OP_€$) are measured as a function of the operating conditions (T, v) by a mechanistic model.

4. Results and discussion

4.1. Comparison of adsorption results of 3 VOCs – ACV 404 carbon

The adsorption capacities of acetone, ethyl formate and dichloromethane are found to be 23.6, 30.3 and 35.6% (based on mass of VOC adsorbed on the activated carbon ACV 404) respectively from the adsorption cycle. And the breakthrough time for acetone; ethyl formate and dichloromethane are found to be 53, 71 and 70 min and it is calculated from 10% of the initial concentration of VOC. The mass transfer coefficients of dichloromethane – ACV404, ethyl formate – ACV404 and acetone – ACV404 systems (D_{gl}) are adjusted as 0.009, 0.003 and 0.001 m^2 s^{-1} respectively. An example of breakthrough curve and temperature profile of ethyl formate during adsorption has been given in Figs. 2 and 3. The simulation model PROSIM results were coherent with the experimental results and it is evident from the Figs. 2 and 3. The error calculated on the mass of adsorption between the experiment and the simulation were always less than 4% for all the VOCs involved. The error on reproduction of data is always 5% on the adsorption capacity for different VOCs.

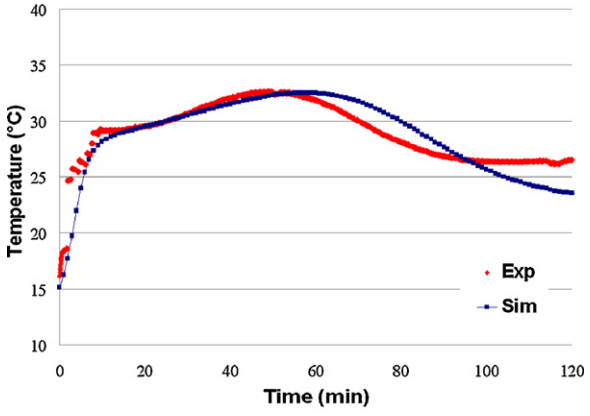

Fig. 3. Ethyl formate adsorption temperature profile of experiment and simulation.

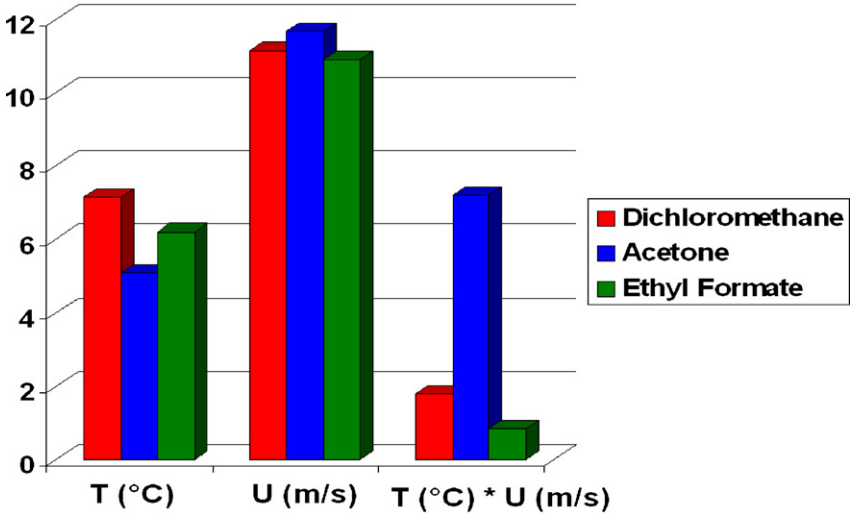

Fig. 4. FED measure of influence of operating conditions on regeneration efficiency.

Table 2
Characteristics of the activated carbon ACV 404.

Activated carbon	Micro pore size (nm)	Bulk density (mg L^{-1})	Micro pore volume ($cm^3\ g^{-1}$)	BET surface area ($m^2\ g^{-1}$)	Total volume ($cm^3\ g^{-1}$)
ACV 404	0.67	0.53	0.54	1256	0.60

Table 3
Ethyl formate regeneration operating conditions and experimental results.

Regeneration experiments	Operating conditions		Regeneration %	Operating cost
	T (°C)	V ($m\ s^{-1}$)	R_E %	$OP_€$ (€/kg)
Reg.1	170 (+)	0.17 (+)	80.0	4.47
Reg.2	170 (+)	0.10 (−)	56.6	3.83
Reg.3	130 (−)	0.17 (+)	66.0	4.91
Reg.4	130 (−)	0.10 (−)	45.9	4.73
Reg.5	150 (=)	0.14 (=)	61.1	4.42

Table 4
Acetone regeneration operating conditions and experimental results.

Regeneration experiments	Operating conditions		Regeneration %	Operating cost
	T (°C)	V ($m\ s^{-1}$)	R_E %	$OP_€$ (€/kg)
Reg.1	170 (+)	0.17 (+)	81.7	5.77
Reg.2	170 (+)	0.10 (−)	57.1	7.60
Reg.3	130 (−)	0.17 (+)	48.2	6.03
Reg.4	130 (−)	0.10 (−)	44.0	6.59
Reg.5	150 (=)	0.14 (=)	56.8	6.48

Table 5
Dichloromethane regeneration operating conditions and experimental results.

Regeneration experiments	Operating conditions		Regeneration %	Operating cost
	T (°C)	V ($m\ s^{-1}$)	R_E %	$OP_€$ (€/kg)
Reg.1	170 (+)	0.17 (+)	84.8	3.44
Reg.2	170 (+)	0.10 (−)	58.9	3.31
Reg.3	130 (−)	0.17 (+)	66.9	4.35
Reg.4	130 (−)	0.10 (−)	48.2	4.04
Reg.5	150 (=)	0.14 (=)	66.5	3.68

4.2. Comparison of hot nitrogen regeneration results of 3 VOCs – ACV 404 carbon

Tables 3–5 summarizes the hot nitrogen regeneration operating conditions and the results (such as regeneration efficiency (RE), Operating Cost (OP€)) for ethyl formate, acetone and dichloromethane respectively. The regeneration efficiency was calculated by the ratio of mass of VOC generated to the mass of the VOC adsorbed. The operating cost was calculated on the basis of the nitrogen consumption (0.18 € m^{-3}, Supplier – Air Liquide) and the energy costs for heating nitrogen (60 € Mwh^{-1}, French electricity tariff). The heat added to nitrogen is calculated by the product of mass flow of nitrogen [m] (kg h^{-1}), specific heat capacity of nitrogen [c_p] (KJ $kg^{-1}\ K^{-1}$) and temperature [ΔT] (K). The efficiency of the heating system is taken into account as 75% from the manufacturer. This energy is applied for 1 h regeneration time and the heating costs could be evaluated with the price of electricity (60 € MWh^{-1}). The mechanistic models for evaluating regeneration efficiency (RE) and the operating costs (OP€) obtained by doing an ANOVA with the MINITAB software. The same approach has been implemented to the other VOCs such as dichloromethane and acetone and the results of FED equation for each VOC are presented as follows:

For acetone – ACV 404 system:

$$R_E\% = 57.8 + 7.2.T + 11.65.v + 5.1.T.v \quad (9)$$

$$OP_{€(€/kg)} = 6.5 - 0.6.T + 0.2.v - 0.3.T.v \quad (10)$$

For ethyl formate – ACV 404 system:

$$R_E\% = 62.1 + 6.2.T + 10.9.v + 0.8.T.v \quad (11)$$

$$OP_{€(€/kg)} = 4.5 - 0.34.T + 0.21.v + 0.11.T.v \quad (12)$$

For dichloromethane – ACV 404 system:

$$R_E\% = 64.7 + 7.2.T + 11.2.v + 1.8.T.v \quad (13)$$

$$OP_{€(€/kg)} = 3.79 - 0.41.T + 0.11.v - 0.05.T.v \quad (14)$$

The error on reproduction of data is always 10% on the regeneration efficiency of different VOCs. In Tables 3–5 regeneration experiment Reg.5 had the operating conditions in the central point of FED (T = 150 °C, v = 0.136 m s^{-1}). The experimental results were compared with the mechanistic models (Eq. (9)) and the error percentage of the mass of regeneration of all VOC is always less than

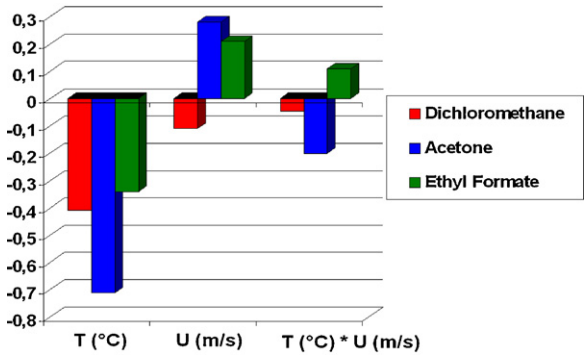

Fig. 5. FED measure of influence of operating conditions on operating costs.

6%. This shows that the mechanistic model is statistically and realistically consistent within the range of operating conditions chosen. So the Eqs. (9)–(14) could be used to interpolate the regeneration efficiency and the operating costs for the different families of VOCs.

Figs. 4 and 5 are plotted by taking the dimensionless coefficients (from Eqs. (9) to (14)) of the corresponding operating conditions (T, v) and their interaction effect ($T \times v$) to compare their influence on regeneration efficiency and operating costs for different VOCs. From the Fig. 4, it could be concluded that the superficial velocity of the nitrogen (v) has influenced more on achieving higher regeneration than the nitrogen temperature (T) for all the VOCs. And also the interaction effect is significantly stronger for the case of acetone compared to dichloromethane and ethyl formate. From the Fig. 5, it could be concluded that the increase in temperature of nitrogen has decreased the operating cost for all the cases of VOCs. This was due to the fact of increasing the temperature had increased the regeneration of VOCs and decreased the regeneration time. The decrease in regeneration time has strictly implied less consumption of nitrogen. And the increase in superficial velocity decreased the operating cost, where as it slightly increased the cost for acetone and ethyl formate. The interaction effect in the case of acetone has decreased the operating cost significantly in case of acetone compared to the case of dichloromethane and ethyl formate.

4.3. Simulation results of the hot nitrogen regeneration step

An example of simulation results of regeneration concentration and temperature profile of ethyl formate have been shown in the Figs. 6 and 7. The average error percent of the mass of acetone regenerated between the simulations and the experiments was 3.1%. It had been noticed in Fig. 6, there has been a delay in the regeneration concentration profile of the experimental in comparison with the simulation results. This was due to the fact of

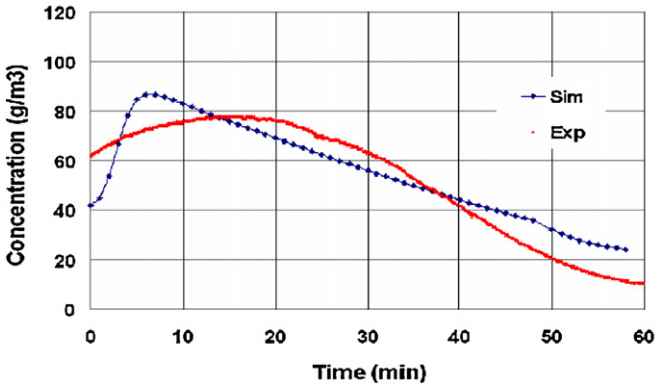

Fig. 6. Regeneration concentration profile of ethyl acetone at 170 °C and 0.17 m s^{-1}.

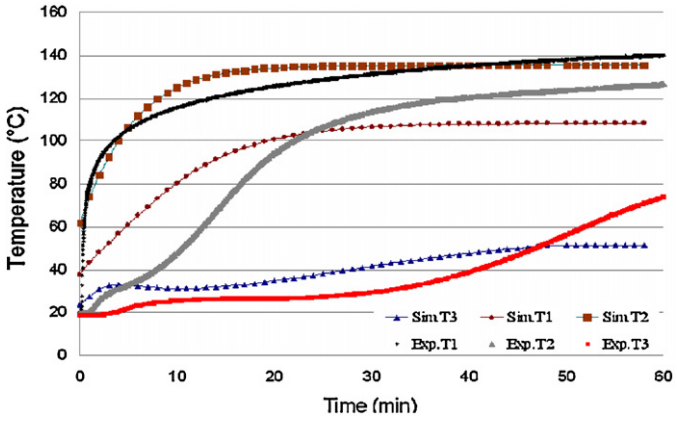

Fig. 7. Regeneration temperature profile of ethyl formate at 170 °C and 0.17 m s^{-1}.

overestimation of the effective mass transfer coefficient of solid to gas (K) in the simulation model. The adjustable effective mass transfer coefficient (K) had been optimized to the best fit of the simulation curve. There were T1, T2, and T3 thermocouples which have recorded at the 4 ports of the column (at x = 2, 19 and 25 cm). The simulation and the experimental readings are marked are 'Exp' and 'Sim' respectively in the above Fig. 7. In Fig. 7, the rise in temperature profile in the simulation was faster than in the experiment. This behavior explains the delay in the regeneration concentration profile of the experiment in comparison with the simulation.

5. Conclusions

The hot nitrogen regeneration operating condition (T = 170 °C; v = 0.17 m s^{-1}) was very effective for the VOCs involved (acetone, ethyl formate and dichloromethane) to achieve high regeneration at an optimized cost. Thanks to the FED tool which has played a very important role in the art of designing and optimizing the state-of-art hot nitrogen regeneration process (TSA). Comparison on the different families of VOC regeneration were analyzed in a detailed fashion that how each operating condition and their interaction effect contributed to the regeneration efficiency and the operating cost. The dynamic systems of adsorption and regeneration had been simulated and validated with the experimental results. The simulation tool had been very useful in (1) choosing the right microporous activated carbon; (2) optimizing the design aspects of adsorption and regeneration process (2) techno-economic analyses (3) analysing security risks in the event of bed fires.

Acknowledgments

The authors acknowledge the French Environment and Energy Management Agency ADEME for their excellent scientific collaboration and for funding the research work.

References

[1] J. Read, D. Whiteoak, S. Bitumen, The Shell Bitumen Handbook, fifth ed., Thomas Telford publishers, London, 2003.
[2] EUR-lex. Access to European law. Directive 1907/2006/EC of the European Parliament and of the Council, December 2006, http://eur-lex.europa.eu/LexUriServ/LexUriServ.do?uri=CELEX:32006R1907:en:NOT.
[3] S. Giraudet, Exothermicity of adsorption of VOCs on activated carbon: modelisation and experimental work, France, Ph.D. Thesis, Ecole des Mines de Nantes, 2006.
[4] P. Pre, F. Delage, P. Le Cloirec, A model to predict the adsorber thermal behavior during treatment of volatile organic compounds onto wet activated carbon, ACS – Environ. Sci. Technol. 36 (2002) 4681–4688.
[5] F. Delage, P. Pre, P. Le Cloirec, Mass transfer and warming during adsorption of high concentrations of VOCs on an activated carbon bed: experimental and theoretical analysis, ACS – Environ. Sci. Technol. 34 (2000) 1172–1185.

[6] P. Pre, F. Delage, P. Le Cloirec, Modeling the exothermal nature of V.O.C. adsorption to prevent activated carbon bed ignition, Fundam. Adsorpt. 7 (2001).
[7] K.S. Hwang, D.K. Choi, S.Y. Gong, S.Y. Cho, Adsorption and thermal regeneration of methylene chloride vapor on activated carbon bed, Chem. Eng. Process. 46 (1998) 1111–1123.
[8] P.M. Berthouex, L.C. Brown, Statistics for Environmental Engineers, second ed., Lewis Publishers, New York, 2002.
[9] J.F. Nastaj, B. Ambrożek, J. Rudnicka, Simulation studies of a vacuum and temperature swing adsorption process for the removal of VOC from waste air streams, Int. Commun. H&M Transfer 33 (2006) 80–86.
[10] S. Giraudet, P. Pre, P. Le Cloirec, Modeling the heat and mass transfer in temperature swing adsorption of volatile organic compounds on to activated carbons, ACS – Environ. Sci. Technol. 43 (2009) 1173–1179.
[11] S.G. Ramalingam, J. Saussac, P. Pré, S. Giraudet, L. Le Coq, P. Cloirec, S. Nicolas, O. Baudouin, S. Déchelotte, A. Medevielle, Hazardous dichloromethane recovery in combined temperature and vacuum pressure swing adsorption process, J. Hazard. Mater. 198 (2011) 95–102.
[12] S.G. Ramalingam, P. Pré, S. Giraudet, L. Le Coq, P. Cloirec, O. Baudouin, S. Déchelotte, Recovery comparisons – hot nitrogen vs steam regeneration of toxic dichloromethane from activated carbon beds in oil sands process, J. Hazard. Mater. 205–206 (2012) 222–228.
[13] J.H. Maindonald, Using R for Data Analysis and Graphics, Introduction, Code and Commentary, R-Stat, 2011, http://cran.r-project.org/doc/contrib/usingR.pdf.
[14] S.G. Ramalingam, L. Hamon, P. Pré, S. Giraudet, L. Le Coq, P. Cloirec, Global statistical predictor model for characteristic adsorption energy or organic vapors–solid interactions: use in dynamic process simulation, J. Colloid Interface Sci., in press.
[15] S. Giraudet, P. Pre, H. Tezel, P. Le Cloirec, Estimation of adsorption energies using physical characteristics of activated carbons and VOCs molecular properties, Carbon 44 (2006) 1873–1883.
[16] J. Keller, R. Staudt, Gas Adsorption Equilibria. Universitat Siegen, third ed., Springer, New York, 1994.
[17] D.M. Ruthven, Principles of Adsorption and Adsorption Processes, second ed., John Wiley & Sons, New York, 1984.
[18] T. Jayabalan, Study of oxidation of carbon materials, Ph.D. Thesis, Ecole des Mines de Nantes, France, May 2008.